# Supporting Information

## Effect of Thermal and Structural Disorder on the Electronic Structure of Hybrid Perovskite Semiconductor $CH_3NH_3PbI_3$

Shivam Singh[a†], Cheng Li[b†], Fabian Panzer [c,d], K. L. Narasimhan[e], Anna Graeser[b], Tanaji P. Gujar[f], Anna Köhler[c], Mukundan Thelakkat[f], Sven Huettner[b*] and Dinesh Kabra[a*]

a. Department of Physics, Indian Institute of Technology Bombay, Powai, Mumbai (India) – 400076
b. Organic and Hybrid Electronics - Macromolecular Chemistry I, Universität Bayreuth, 95440, Germany.
c. Experimental Physics II & Bayreuth Institute of Macromolecular Research (BIMF), Universität Bayreuth, 95440, Germany.
d. Department of Functional Materials, Universität Bayreuth, 95440, Germany.
e. Department of Electrical Engineering, Indian Institute of Technology Bombay, Powai, Mumbai (India) – 400076
f. Applied Functional Polymers - Macromolecular Chemistry I, Universität Bayreuth, 95440, Germany.

† Authors contributed equally.

**UV-Vis Spectrum analysis**:

In order to determine the electronic bandgap and excitonic properties of these materials we model our experimental results using Elliot's theory of Wannier exciton in 3D semiconductors. The following equation is used to fit measured UV-Vis spectrums of $CH_3NH_3PbI_3$ films:

$$\alpha(E) \propto \frac{\mu^2}{E}\left[\sum_n \frac{2E_x}{n^3} sech\left(\frac{E-E_n^x}{\Gamma}\right) + \int_{E_g}^{\infty} sech\left(\frac{E-E_n^x}{\Gamma}\right) \frac{1}{1-e^{-2\pi\sqrt{E_x/E_1-E_g}}} \frac{1}{1-\frac{128\pi\mu b}{\hbar}(E_1-E_g)} dE_1\right]$$

Where $E_x$, μ, Γ, E and b are exciton binding energy, transition dipole moment, FWHM of excitonic peak, photon energy and non-parabolic contribution, respectively. This equation is valid for bulk semiconductors with $E_x$ much smaller than the $E_g$ (Wannier excitons) and was used to describe optical transitions to bound and/or ionized excitonic states in model inorganic semiconductors. In above equation there are two terms, first term represents excitonic levels below the conduction band of various perovskite semiconductors and second terms represents the continuum of states beyond the energy of $E_g$ as band-to-band transition contribution in the overall optical absorption. The absorption in the continuum spectrum does not simply resemble a square root dependence of the density of states on energy $\alpha(h\nu)^2 = A(E-E_g)$ as expected for bare band-to-band transitions between uncorrelated electrons and holes. The excitonic enhancement of the optical density of states at band-edge depends on the strength of the Coulomb interaction, through the exciton binding energy and reflects the strength of their correlation.[1]

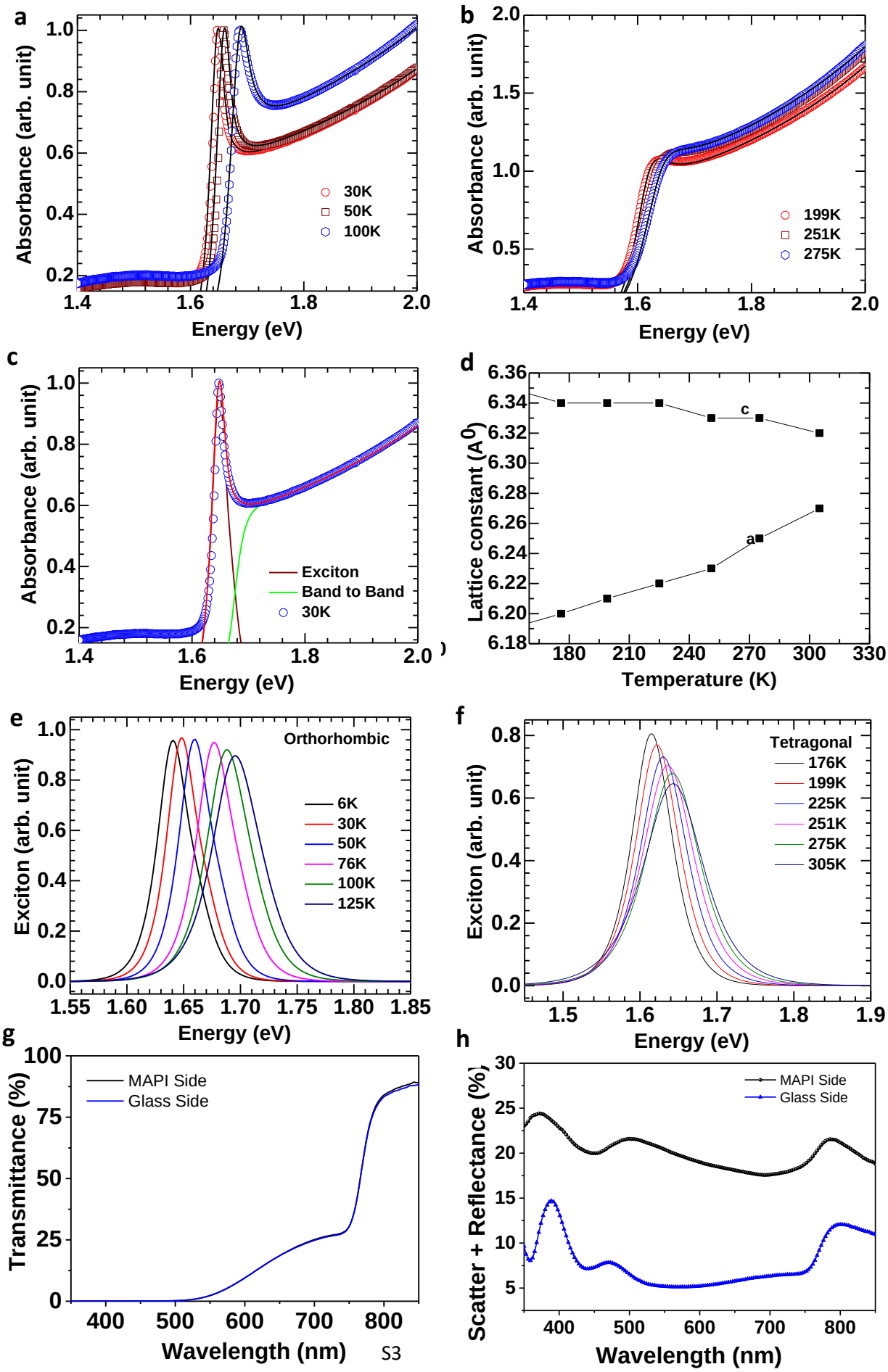
a
Absorbance (arb. unit)
Energy (eV)
30K
50K
100K
b
Absorbance (arb. unit)
Energy (eV)
199K
251K
275K
c
Absorbance (arb. unit)
Energy (eV)
Exciton
Band to Band
30K
d
Lattice constant (A0)
Temperature (K)
c
a
e
Exciton (arb. unit)
Energy (eV)
Orthorhombic
6K
30K
50K
76K
100K
125K
f
Exciton (arb. unit)
Energy (eV)
Tetragonal
176K
199K
225K
251K
275K
305K
g
Transmittance (%)
Wavelength (nm)
MAPI Side
Glass Side
h
Scatter + Reflectance (%)
Wavelength (nm)
MAPI Side
Glass Side

**Figure S1:** UV-Vis absorption spectra of $CH_3NH_3PbI_3$ thin film at different temperatures: (a) Orthorhombic (b) Tetragonal phase of $ABI_3$. Black solid line is fit to the experimental absorption spectra (Scatter points). (c) UV-Vis absorption spectra of $CH_3NH_3PbI_3$ at 30K. Red line is fit to the experimental absorption spectra (blue scatter points), where wine and olive line represents the exciton and band to band contributions respectively. (d) Variation of lattice constant with temperature (adapted from[2]). (e) Excitonic contribution in orthorhombic phase and (f) in tetragonal phase, visualizing the broadening with higher temperature. (g,h) transmittance, scatter and reflectance measured with an integrating sphere showing that a certain amount of scattering is involved with these samples.

Fitting of Variation of exciton FWHM with temperature [Fig S2(a)]

$$\Gamma(T) = \Gamma_0 + \frac{\Gamma_{ep}}{exp\left(\frac{E_P}{K_B T}\right) - 1}$$

Where, $\Gamma_0$= intrinsic linewidth at T=0K = (11.45±0.21) meV

$\Gamma_{ep}$ = coupling constant =(14.55±1.67)meV

$E_P$ = LO phonon energy = (13.14±1.21) meV

Here, $k_B$= 8.61X $10^{-2}$ meV/K

Results from the fitting of Fig S2 (b)

$\sigma_0$ = (0.433±0.009) ; $h\nu_p$ = (20.58±1.13) meV

Results from fitting of Fig S2 (c)

Θ = Einstein Characteristic Temperature = (223±19) K

P = Structural Disorder = (0.017±0.0.05)

N = Thermal Phonon Interaction Term = 1 (Fixed)

$E_u$ (T=0K) = 21.47 meV $E_u$(T=305K)= 58.72 meV

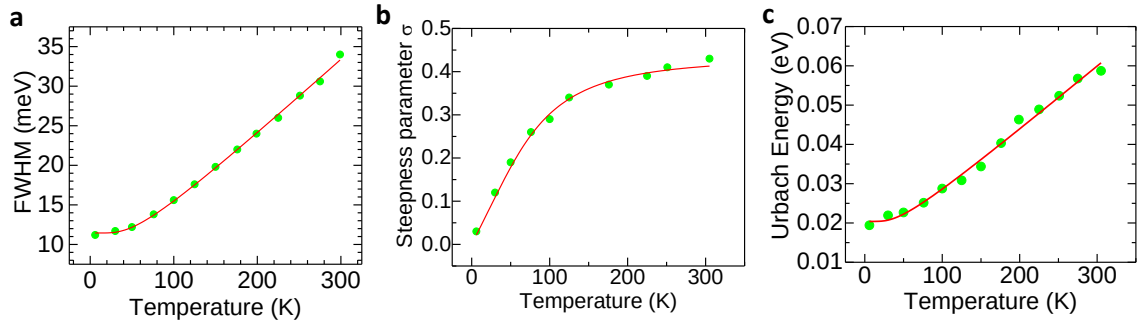


**Figure S2**: (a) Variation of FWHM of excitonic peak with temperature in $CH_3NH_3PbI_3$. (b) Steepness parameter as a function of temperature for $CH_3NH_3PbI_3$. (c) Urbach energy as a function of temperature for $CH_3NH_3PbI_3$. Red solid line is fit to the experimental data. Fittings are done without separating phases of $CH_3NH_3PbI_3$.

## Volume expansion coefficient of $MAPbI_3$

The volume expansion coefficient was determined by plotting ln(V) against T(K) and using the slope of the linear fit (Figure S3). The volume for the tetragonal cell was calculated after: $V = a^2 * c$

For comparison Kawamura et al.[3] calculated the volume after the same equation where **a** was calculated from $\tilde{a} = a / \sqrt{2}$ and **c** from $\tilde{c} = c/2$.

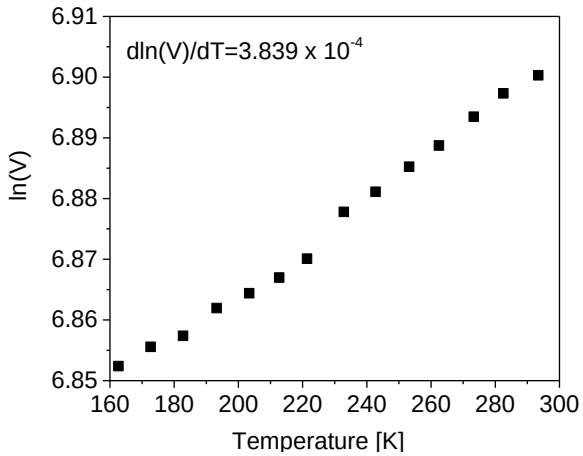


**Figure S3:** Thermal expansion within the tetragonal phase during cooling (approx. 10K/min).

For the orthorhombic cell the volume was calculated after V=a*b*c (Figure S4).

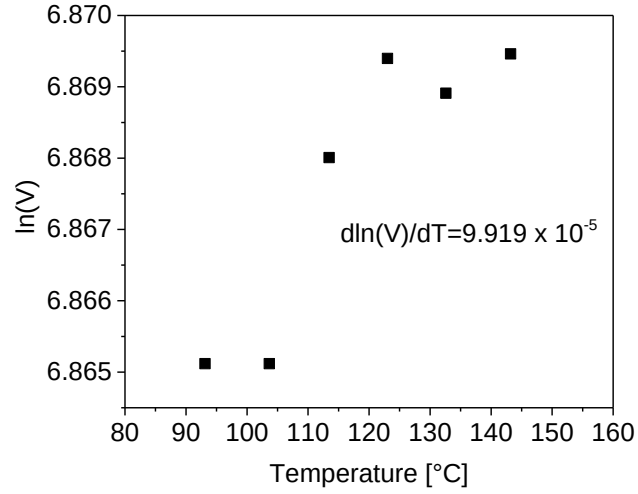


**Figure S4:** Thermal expansion within the orthorhombic phase within the heating cycle (approx. 10K/min)

**Photoluminescence:**

High energy side of the PL of the orthorhombic phase was fitted for temperatures <120K using a superposition of an exponential decay and a Gaussian:

$$y = y_0 + A * e^{-\frac{x-x_0}{t_1}} + \left(\frac{B}{w\sqrt{\pi/2}}\right) e^{-2\left(\frac{x-x_C}{w}\right)^2}$$

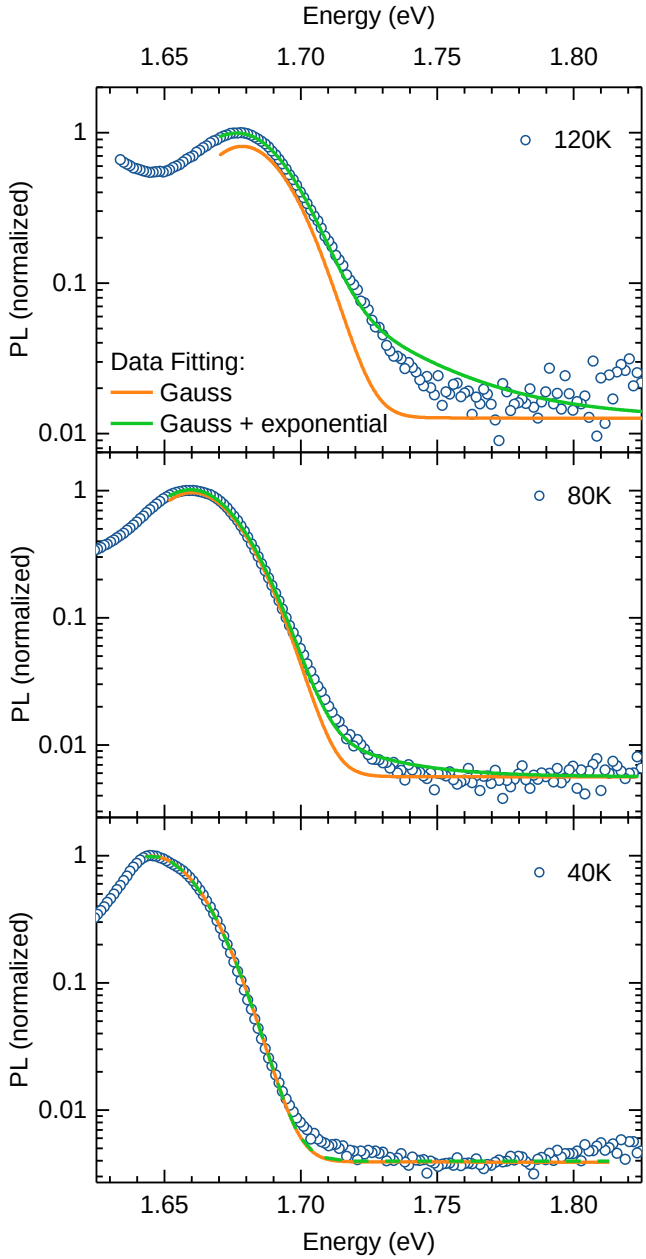


**Figure S5**: PL spectra at 120K (top), 80K (middle) and 40K (bottom) together with best fits of the high energy side of the spectra using either a superposition of a Gaussian and an exponential (green line) or only a Gaussian (orange line).

**Stokes Shift approach:**

By calculating the difference between the temperature dependent energetic positions of the PL peak and the already determined excitonic peak from the absorption data (Figure 2), we obtain the temperature dependent Stokes shift (Figure S6).

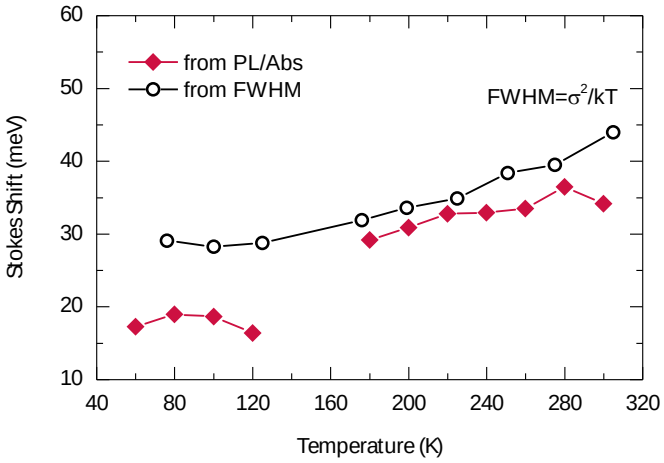


**Figure S6**: Calculated stokes shift form peak positions of the excitonic absorption peak and the photoluminescence peak (red symbols). The spectral diffusion calculation is given by the black open symbols.

Within the tetragonal phase (300 K – 160 K) values are in the range of 30 - 35 meV and in the orthorhombic phase (< 160 K) in the range between 15-20 meV

It is known that, besides other parameters, the Stokes shift correlates with the degree of disorder in the material. As already established above, the structural disorder is small in both phases, which leads only to a small Stokes shift that we observe in our data in the entire temperature range investigated. To further investigate to which extend the observed Stokes shift can be attributed toward the small amount of disorder in the material, we fit the data set with a spectral diffusion term. Spectral diffusion is the diffusion of excited states through various energy sites at a given temperature. Assuming a Gaussian distribution of energy levels of the excitons with the width $\Gamma_{EX}$, the difference between the PL and exciton absorption peak (Stokes shift) at given T is given by[2]:

$$\Delta\epsilon = \frac{\sigma\,{\Gamma_{EX}}^2}{kT}$$

The slope as well as the absolute values of the Stokes shift match well within the temperature range of the tetragonal phase, we therefore attribute the Stokes shift in the tetragonal phase to be a consequence of the disorder in the material, which possibly can stem from a distribution of trap states and/or a distribution of excitonic active areas with different sizes within single grains. In contrast to the tetragonal phase, for temperatures below the phase transition the values $\Delta\epsilon$ which were

calculated based on the FWHM of the PL Peaks seem to overestimate the Stokes shift by about 10-15 meV. While the detailed explanation and analysis on this difference is beyond the scope of this work, it nevertheless shows the higher order in the orthorhombic phase due to the experimentally obtained small Stokes shift at temperatures below the phase transition.

**Quality of Perovskite conversion**

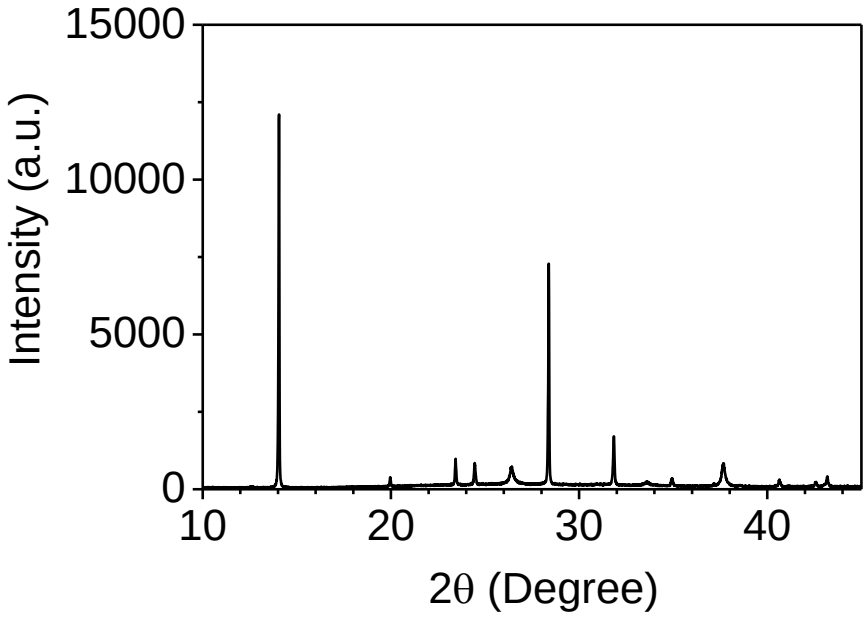


**Figure S7**: XRD spectra of the $MAPbI_3$ sample, confirming the full conversion of $PbI_2$ using MAI vapour assisted perovskite processing.

[1] Saba, M. *et al.* Correlated electron–hole plasma in organometal perovskites. Nat. Commun. **5**, 5049, (2014)
[2] Kawamura, Y., Mashiyama, H. & Hasebe, K. Structural study on cubical-tetragonal transition of $CH_3NH_3PbI_3$. *J Phy. Soc. Jpn.* **71**, 1694 (2002)
[2] Hoffmann, S. T. *et al.* Spectral diffusion in poly(para-phenylene)-type polymers with different energetic disorder. *Phys. Rev. B* **81**, 11510 (2010)